

Potassium under Pressure: A Pseudobinary Ionic Compound

M. Marqués, G. J. Ackland, L. F. Lundegaard, G. Stinton, R. J. Nelmes, and M. I. McMahon

SUPA, School of Physics and Astronomy and Centre for Science at Extreme Conditions, The University of Edinburgh, Mayfield Road, Edinburgh, EH9 3JZ, United Kingdom

J. Contreras-García

Department of Chemistry, Duke University, Durham, North Carolina 27708, USA

(Received 7 June 2009; published 8 September 2009)

Experimentally, we have found that among the “complicated” phases of potassium at intermediate pressures is one which has the same space group as the double hexagonal-close-packed structure, although its atomic coordination is completely different. Calculations on this $P6_3/mmc$ ($hP4$) structure as a function of pressure show three isostructural transitions and three distinctive types of chemical bonding: free electron, ionic, and metallic. Interestingly, relationships between localized metallic structures and ionic compounds are found.

DOI: 10.1103/PhysRevLett.103.115501

PACS numbers: 61.50.Ks, 62.50.-p, 71.20.-b

It is becoming strikingly clear that the free-electron model of simple metals is not applicable when metals are compressed. A deviation from “ideal” metallic behavior is observed for all group 1 and 2 elements at intermediate pressures, manifested by the appearance of open and/or incommensurate structures with unusual properties such as decreased conductivity, low melting points, and superconductivity [1]. This challenging state of matter has been explained in terms of Peierls distortions, Fermi surface–Brillouin zone interactions, $s \rightarrow p$ or $s \rightarrow d$ electronic transitions, and an increase of valence electron density in interstitial regions [2]. The localization and reduction in metallicity in groups 1 and 2 under pressure contrasts sharply with the delocalization and increasing metallicity observed in groups 3–7 [3].

Potassium, like the other alkali metals, adopts the body-centered-cubic (bcc) crystal structure at ambient pressure, becoming face-centered-cubic (fcc) at 11 GPa. It then transforms through a sequence of composite host-guest structures before adopting the orthorhombic $oP8$ structure between 54–90 GPa [4,5].

We have collected further room temperature x -ray powder diffraction data from a high-purity potassium sample contained in a diamond anvil cell (Fig. 1). The previously reported transitions through incommensurate phases [4,5] were seen in six samples. However, in two samples a different phase was observed between 25 and 35 GPa. A diffraction pattern from this phase at 25 GPa, and its Rietveld refinement, are shown in Fig. 1. This phase is hexagonal, spacegroup $P6_3/mmc$, with 4 atoms per unit cell located on the $2a$ and $2c$ sites at $(0, 0, 0)$ (K_1) and $(\frac{1}{3}, \frac{2}{3}, \frac{1}{4})$ (K_2), respectively. The lattice parameters at 25 GPa are $a = 4.2180(5)$ Å and $c = 5.7369(3)$ Å, with a c/a ratio of 1.3601(2). This is the same $hP4$ structure recently reported for the transparent, insulating phase of Na observed above 200 GPa [6], that is, at pressures *above* the stability range of the $oP8$ phase of Na.

The double hexagonal-close-packed (dhcp) structure, which has the same spacegroup and atomic positions as $hP4$, has been proposed as the stable structure of K and Rb at extreme compression (above 250 and 143 GPa, respectively) [7], and is observed in Cs from 72 GPa to at least 184 GPa. This reappearance of the hexagonal structure has similarities with Ba [8] where hcp is a reentrant phase and the intermediate instability is associated with incommensurate phases. However, the proposed dhcp structures in K, Rb, and Cs have c/a ratios near to the $ABAC$ close packing $2\sqrt{8/3} = 3.266$, very different from the c/a ratio of 1.46 and 1.36 observed in $hP4$ Na and K, respectively. So the $hP4$ structures of Na and K would not be regarded as close-packed.

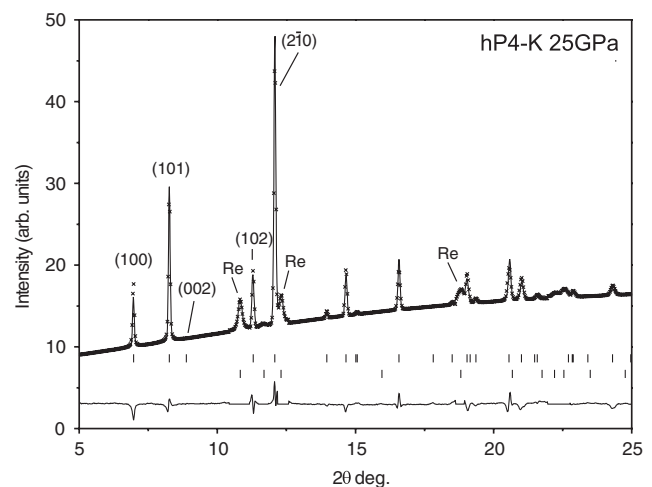


FIG. 1. Rietveld refinement of $hP4$ -K at 25 GPa. Tick marks show calculated peak positions of (upper) the $hP4$ phase and (lower) the Re gasket. The difference between observed (crosses) and calculated (line) profiles is shown beneath the tick marks. Some low-angle reflections are indexed. We used beam line 9.5HPT at the SRS synchrotron, Daresbury Laboratory, with an x -ray wavelength of 0.443 97 Å.

The *oP8* phase observed in K is a distortion of the *hP4* structure, involving the freezing of a symmetry-breaking phonon and associated orthorhombic cell distortion. Similar transitions between *oP8*-like and *hP4*-like structures (with c/a ratios of approximately 1.36) occur in di-alkali-metal monochalcogenides and their oxides. Calculation of the electronic structure reveals a relationship between K under pressure and these ionic compounds.

We calculated the enthalpy of potassium at pressure within the density-functional theory formalism with a plane-wave pseudopotential approach, using the VASP code [9]. We used the Perdew-Burke-Ernzerhof (PBE) exchange-correlation functional [10] and the projector augmented wave description of the electron-ion-core interaction [11]. Brillouin zone integrals were converged with plane-wave cutoff (390 eV) and k -point density (18^3 meshes [12], using the tetrahedron method with Blöchl correction). The calculated energies neglect zero point vibrational contributions.

The evolution of the calculated c/a ratio and the distances around the unoccupied $2d$ site of the *hP4* structure from 0 to 200 GPa are shown in Figs. 2(a) and 2(b). There are four well-differentiated regions. At low and high pressures (below 20 GPa and above 85 GPa), the c/a ratio approaches the close-packing value of 3.266. But in the pressure range 20–50 GPa, in which we observed *hP4* experimentally, the c/a ratio is very close to the experimental value of 1.36 and the distances from the $2d$ interstitial site (see below) to the neighboring atoms increase significantly. In the third pressure region, 50–85 GPa, in which we see the *oP8* phase experimentally, the c/a value evolves continuously from 2.0 to 2.3.

The atomic arrangement in the *hP4* structure in the 20–50 GPa pressure range is the same as that of the cations in the Ni_2In -type structures of several di-alkali-metal monochalcogenides and their corresponding sulfates, such as Na_2S , Rb_2Te , Na_2SO_4 , and K_2SO_4 . And the c/a ratios of these structures (1.31, 1.29, 1.34, and 1.37, respectively) are also very similar to those observed here. The anions in these structures occupy the interstitial $2d$ ($\frac{1}{3}, \frac{2}{3}, \frac{3}{4}$) site, unoccupied in the *hP4* structure of K. Di-alkali-metal dichalcogenides, where the arrangement of the cations again forms the *hP4* structure, have similar c/a ratios to those calculated for K in the 50–85 GPa region: e.g., Li_2O_2 ($c/a = 2.42$), Na_2Se_2 ($c/a = 2.25$), and K_2Te_2 ($c/a = 2.18$). This can be explained through the anions in the metallic matrices model (AMM) for ionic compounds: a metallic matrix acts as a host lattice for the nonmetallic atoms, the formation and localization of the anions being determined by the geometric and electronic structure of the metallic sublattice [13]. AMM can be applied to elemental potassium by treating it as an electride: rather than being associated with atoms, the valence electrons are localized in interstitial positions, which we refer to as pseudoanions.

The discontinuities in Figs. 2(a) and 2(b) correspond to the phase transitions observed experimentally. Below

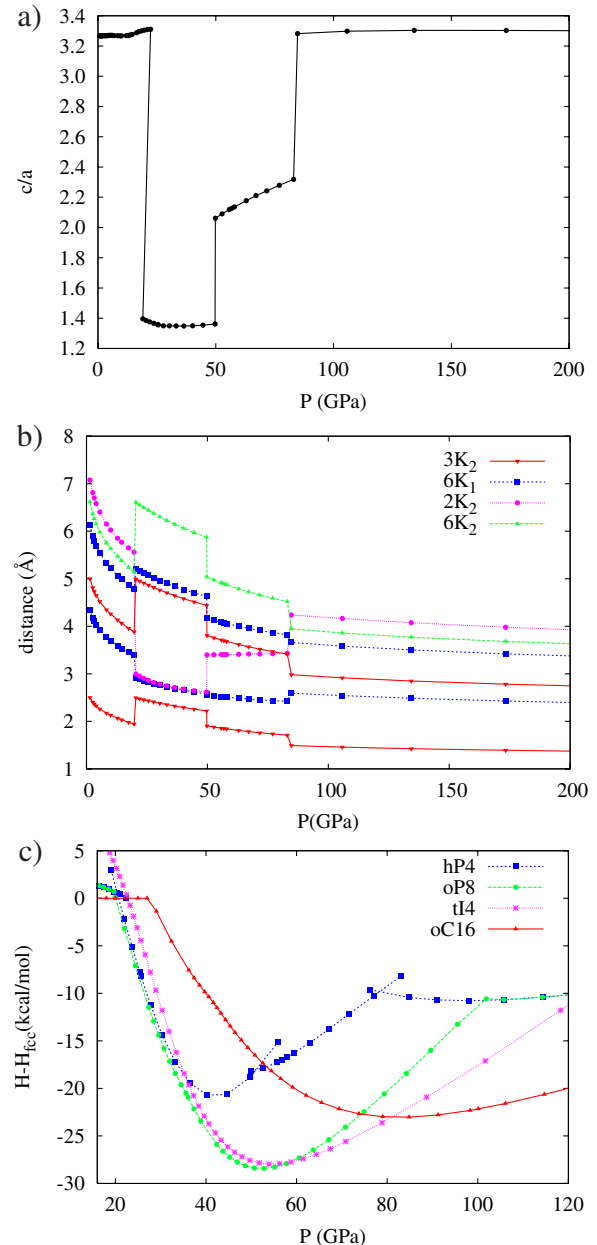


FIG. 2 (color online). Calculated (a) c/a ratio and (b) distances from the $2d$ ($\frac{1}{3}, \frac{2}{3}, \frac{3}{4}$) site of the *hP4* structure to the adjacent atoms versus pressure, where nK_b means n potassium atoms of b type. (c) Enthalpy versus pressure for a range of possible structures in K.

20 GPa the “ideal” c/a ratio mirrors the free-electron bcc and fcc structures. The second region, between 20 and 50 GPa, corresponds to that in which incommensurate phases and the *hP4* structure are observed, while the region between 50 and 85 GPa marks the transition to the pseudohexagonal *oP8* phase. The final discontinuity at 85 GPa relates to the observed transition to the *tI4* and *oC16* phases (a slight distortion from close-packed fcc), and also anticipates the predicted stabilization of the *dhcp* structure at very high pressures [7].

Thus the *hP4* structure can be a close analogue of many of the observed phases of K: all the electronic transition types are present in the single symmetry group. This suggests that details of the observed crystal symmetries are secondary to electronic structure in understanding the physics driving these transitions.

The calculated enthalpy-pressure relation [Fig. 2(c)] shows that at 25–35 GPa where we have observed *hP4* experimentally, it is slightly unstable with respect to *oP8*, which itself is unstable with respect to the incommensurate phases [4]. The phonon spectrum of *hP4*-K [14] (Fig. 3) identifies the M_2^- mode as the relevant order parameter of the transformation: since this soft-mode transition involves a small distortion, it cannot be kinetically hindered. However, higher symmetry structures can be dynamically stabilized by temperature [15], and the transition temperature is typically of order the energy difference between the two structures [16], here $\Delta H/k_B = 97$ K at 27 GPa, well below the experimental temperature of 293 K. With increasing pressure, the *oP8* structure becomes clearly more stable than the *hP4* [Fig. 2(c)] although it is not observed until 54 GPa. Finally, *oP8*-K reverts to the dhcp structure around 95 GPa (see supplementary material [17]).

To investigate the electronic structure we calculated the valence electron localization function (ELF) [18,19] using the CRITIC program [20] and VASP-optimized structures recalculated with CRYSTAL98 [21] using the same PBE functionals. The ELF partitions space into nonoverlapping basins with well-defined chemical interpretation: atomic shells, bonds, and lone pairs. Moreover, the ELF value at the boundary between basins can be used to characterize chemical bonding. Electron pairing (atomic shells, bonds, and lone pairs) gives $\text{ELF} \rightarrow 1$; the delocalized limit (free electron gas) has $\text{ELF} = 0.5$; while $\text{ELF} \rightarrow 0$ is characteristic of interstitial nonbonding regions.

At low pressure the valence ELF values are close to 0.5 everywhere: K is a simple free-electron metal. At 25 GPa we find distinct maxima ($\text{ELF} \approx 0.95$) at the interstitial positions on the *2d* sites. Their basins, comprising $\sim 44\%$ of the cell volume, form well-defined chemical entities holding approximately 2 electrons each (see Fig. 6 in the supplementary material [17]). We identify these with

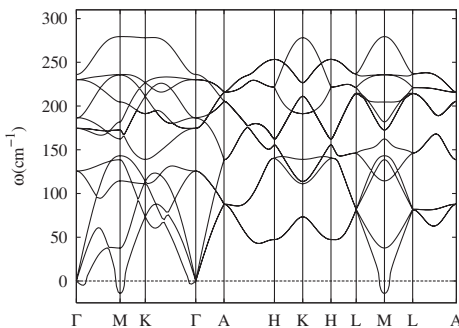


FIG. 3. Phonon spectrum for *hP4* potassium at 26 GPa. *oP8* has lower energy at this pressure, and is related by a symmetry-breaking phonon at the *M* point, $k = (\frac{1}{2}, 0, 0)$.

Lewis pairs that act as pseudoanions. The pseudoionic nature is highlighted by the fact that the position of these X^{2-} pseudoanions coincides with the chalcogen position in the Ni_2In -type compounds. Viewed as an ionic compound, the K_1 atoms are octahedrally coordinated by 6 pseudoanions, with 2 further neighboring K_1 atoms along the *c* axis. The K_2 atoms have 5 neighboring pseudoanions, 3 in-plane and 2 along the *c* axis, forming a triangular bipyramid. The pseudoanions themselves are 11-fold coordinated and adopt an irregular hcp arrangement.

Between 50–85 GPa, the *2d* sites in *hP4* are too small to accommodate pseudoanions. With constrained symmetry, the ELF has an elongated basin and electrons flow towards the *4f* positions ($\frac{1}{3}, \frac{2}{3}, \approx 0.6$), occupied by the anions in the dichalcogenides. This peculiar basin shape hides an intrinsic electronic instability towards the *oP8* phase (see Fig. 7 in the supplementary material [17]). The *oP8* distortion increases the volume of the pseudoanion basin. Since *oP8* is calculated to have lower enthalpy and higher maximal ELF value than the parent *hP4* phase, we conclude that the greater interstitial electronic localization helps to stabilize the *oP8* phase.

Above 85 GPa, the electronic flow is completed and differentiated ELF maxima with metallic values emerge on the *4f* positions, signalling the onset of the dhcp arrangement [see Fig. 7(f) in the supplementary material [17]].

The *hP4* band structure in each of the four regions is shown in Fig. 4. The differences are striking, showing the electronic origins of the isostructural transitions. The low-pressure phase is a classic free-electron-like metal, with the *s* band crossing the Fermi surface [Fig. 4(a)]. At 25 GPa, we predict that *hP4*-K is a semiconductor [Fig. 4(b)]. At 33 GPa the gap closes [Fig. 4(c)], but we still have flat (i.e., well-localized) valence bands occupied at all *k* points: this is contrasted with a putative *hP4* structure of ideal *c/a* ratio at the same volume which retains the free-electron behavior [Fig. 4(d)]. After the transition at 50 GPa, the *hP4* structure still shows flat bands with valence electrons at all *k* points [Fig. 4(e)]. However, if we freeze-in the *oP8* distortion [Fig. 4(f)] there is considerable movement of bands away from the Fermi energy, showing that the soft mode distortion is driven by Fermi surface–Brillouin zone interactions [22,23], although we find no evidence for core electrons participating in the valence bonding (the *3p* band, not shown, lies about 14.8 eV below the Fermi energy). The third transition at 85 GPa reverts to transition-metal-type behavior, with multiple bands crossing the Fermi surface [Fig. 4(g)].

The picture of localized electrons in *hP4* and *oP8* opens the possibility that there may be strong-correlation effects, which are poorly described by PBE exchange. If so, then the *oP8* and *hP4* phases should be more stable than calculated: there is some evidence for this—the calculated *oP8*-*tI4* transition pressure is much lower than observed in K [5], and in Na the experimentally observed *oP8* phase

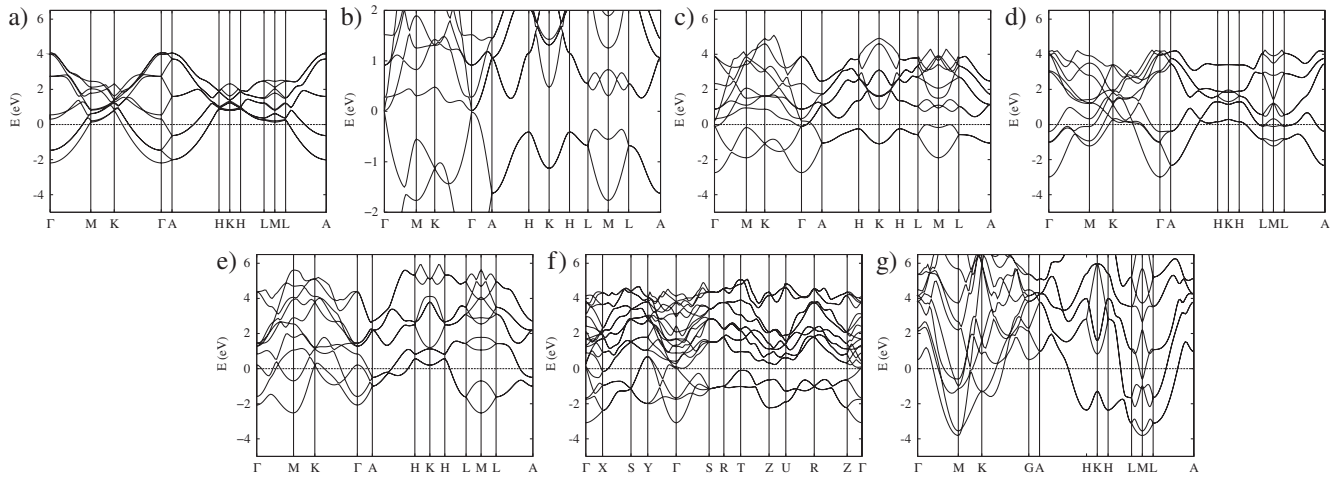


FIG. 4. Calculated band structures of *hP4* potassium. (a) Ambient pressure: free-electron-like. (b) 25 GPa: semiconductor. (c) 33 GPa: flat localized valence bands. (d) 33 GPa with ideal $c/a = 3.266$: unstable and metallic. (e) 57 GPa: flat localized bands. (f) 57 GPa: with *oP8* distortion. (g) 305 GPa: transition-metal-like.

does not have lowest calculated enthalpy [6]. This picture also opens the possibility that *oP8* potassium may be a Mott insulator.

We have observed the *hP4* phase experimentally in K, and calculated its electronic structure as a function of pressure. Within the $P6_3/mmc$ space group we find three distinct types of bonding, delineated by sharp changes in the c/a ratio. At low pressure, we find a conventional simple metal. Above 20 GPa electrons become localized in interstitial sites (pseudoanions) and the material is better thought of as ionic compound (“electride”). Above 50 GPa this electride becomes mechanically unstable with respect to a combined elastic instability and phonon distortion to the observed *oP8* phase that favors further interstitial localization. Above 85 GPa the material reverts to close-packing and metallic behavior.

The experimentally observed sequence of phase transitions in potassium involves changes in spacegroup. However, our study suggests that it is likely that the types of electronic structure we describe are similar. The low-pressure phase is essentially free-electron-like, with the crystal structure determined by weak interionic repulsion. At intermediate pressures, electridelike phases like *hP4*, *oP8*, and likely the composite ones are preferred. Finally, the high-pressure phase has a volume typical of the transition metals, and can be associated with core repulsion and close packing.

We thank A. Lennie of Daresbury Laboratory for setting up the 9.5HPT beam line. This work was supported by grants from the EPSRC, and facilities provided by Daresbury Laboratory.

[1] E. Yu. Tonkov and E. G. Ponyatovsky, *Phase Transformations of Elements Under High Pressure* (CRC, London, 2005).

- [2] B. Rousseau and N.W. Ashcroft, *Phys. Rev. Lett.* **101**, 046407 (2008).
- [3] G.J. Ackland, *Rep. Prog. Phys.* **64**, 483 (2001).
- [4] M.I. McMahon *et al.*, *Phys. Rev. B* **74**, 140102(R) (2006).
- [5] L.F. Lundegaard *et al.*, *Phys. Rev. B* **80**, 020101(R) (2009).
- [6] Y. Ma *et al.*, *Nature (London)* **458**, 182 (2009).
- [7] Y. Ma, A.R. Oganov, and Y. Xie, *Phys. Rev. B* **78**, 014102 (2008).
- [8] S.K. Reed and G.J. Ackland, *Phys. Rev. Lett.* **84**, 5580 (2000).
- [9] G. Kresse and J. Furthmuller, *Phys. Rev. B* **54**, 11 169 (1996).
- [10] J.P. Perdew, K. Burke, and M. Ernzerhof, *Phys. Rev. Lett.* **77**, 3865 (1996).
- [11] G. Kresse and D. Joubert, *Phys. Rev. B* **59**, 1758 (1999).
- [12] H.J. Monkhorst and J.D. Pack, *Phys. Rev. B* **13**, 5188 (1976).
- [13] Á. Vegas *et al.*, *Acta Crystallogr. Sect. B* **62**, 220 (2006).
- [14] Phonons were calculated using the QUANTUM-ESPRESSO code, available at <http://www.quantum-espresso.org>.
- [15] N.D. Drummond and G.J. Ackland, *Phys. Rev. B* **65**, 184104 (2002).
- [16] G.J. Ackland, *J. Phys. Condens. Matter* **14**, 2975 (2002).
- [17] See EPAPS Document No. E-PRLTAO-103-057937 for details of structural parameters and DOS of K-*oP8*, and ELF isosurfaces and planes of K-*hP4*. For more information on EPAPS, see <http://www.aip.org/pubservs/epaps.html>.
- [18] A.D. Becke and K.E. Edgecombe, *J. Chem. Phys.* **92**, 5397 (1990).
- [19] B. Silvi and A. Savin, *Nature (London)* **371**, 683 (1994).
- [20] J. Contreras-García *et al.*, *J. Chem. Theory Comput.* **5**, 164 (2009).
- [21] R. Dovesi *et al.*, <http://www.crystal.unito.it>.
- [22] G.J. Ackland and I.R. Macleod, *New J. Phys.* **6**, 138 (2004).
- [23] V. Degtyereva and O. Degtyereva (unpublished).